energies

Article

Experimental Study on Carbon Dioxide Flooding Technology in the Lunnan Oilfield, Tarim Basin

Zangyuan Wu [1,2], Qihong Feng [1,*], Yongliang Tang [2], Daiyu Zhou [2] and Liming Lian [3]

1 School of Petroleum Engineering, China University of Petroleum (East China), Qingdao 266580, China; wuzy-tlm@petrochina.com.cn
2 PetroChina Tarim Oilfield Company, Korla 841000, China; tangyl-tlm@petrochina.com.cn (Y.T.); zdy-tlm@petrochina.com.cn (D.Z.)
3 Research Institute of Petroleum Exploration and Development, Beijing 100083, China; lianliming@petrochina.com.cn
* Correspondence: fengqihong@upc.edu.cn

Abstract: The Lunnan Oilfield in the Tarim Basin is known for its abundant oil and gas resources. However, the marine clastic reservoir in this oilfield poses challenges due to its tightness and difficulty in development using conventional water drive methods. To improve the recovery rate, this study focuses on the application of carbon dioxide flooding after a water drive. Indoor experiments were conducted on the formation fluids of the Lunnan Oil Formation, specifically investigating gas injection expansion, thin tube, long core displacement, oil and gas phase permeability, and solubility. By injecting carbon dioxide under the current formation pressure, the study explores the impact of varying amounts of carbon dioxide on crude oil extraction capacity, high-pressure physical parameters of crude oil, and phase characteristics of formation fluids. Additionally, the maximum dissolution capacity of carbon dioxide in formation water is analyzed under different formation temperatures and pressures. The research findings indicate that the crude oil extracted from the Lunnan Oilfield exhibits specific characteristics such as low viscosity, low freezing point, low-medium sulfur content, high wax content, and medium colloid asphaltene. The measured density of carbon dioxide under the conditions of the oil group is 0.74 g/cm^3, which closely matches the density of crude oil. Additionally, the viscosity of carbon dioxide is 0.0681 mPa·s, making it well-suited for carbon dioxide flooding. With an increase in the amount of injected carbon dioxide, the saturation pressure and gas-oil ratio of the crude oil also increase. As the pressure rises, carbon dioxide dissolves rapidly into the crude oil, resulting in a gradual increase in the gas-oil ratio, expansion coefficient, and saturation pressure. As the displacement pressure decreases, the degree of carbon dioxide displacement initially decreases slowly, followed by a rapid decrease. Moreover, an increase in the injection rate of carbon dioxide pore volume leads to a rapid initial improvement in oil-displacement efficiency, followed by a slower increase. Simultaneously, the gas-oil ratio exhibits a slow increase initially, followed by a rapid rise. Furthermore, as the displacement pressure increases, the solubility of carbon dioxide in water demonstrates a linear increase. These research findings provide valuable theoretical data to support the use of carbon dioxide flooding techniques for enhancing oil recovery.

Keywords: Lunnan oilfield; carbon dioxide flooding; gas injection expansion; oil and gas phase seepage

check for updates

Citation: Wu, Z.; Feng, Q.; Tang, Y.; Zhou, D.; Lian, L. Experimental Study on Carbon Dioxide Flooding Technology in the Lunnan Oilfield, Tarim Basin. *Energies* **2024**, *17*, 386. https://doi.org/10.3390/en17020386

Academic Editor: Mofazzal Hossain

Received: 31 October 2023
Revised: 6 December 2023
Accepted: 14 December 2023
Published: 12 January 2024

1. Introduction

With the rapid increase in the development of conventional oil reservoirs around the world, the reserves and annual production of conventional oil reservoirs and high-quality oil reservoirs are continuously decreasing [1]. As the reserves and production of tight oil and gas are increasing year by year, it has become the reservoir for global oil and natural gas production [2]. Tight reservoirs are characterized by poor physical properties, small pore throats, and threshold pressure gradients [3]. Through the high injection pressure, the water absorption capacity of the tight reservoir is poor, which leads to the slow development of water injection in oil wells [4]. The Lunnan Oilfield in the Tarim Basin is a low-porosity and low-permeability reservoir with a small pore throat radius, strong heterogeneity, large mud influence, and the development of micro-fractures, which makes overall development difficult [5]. By interacting carbon dioxide with tight oil, the oil displacement mechanism of viscosity reduction, expansion, and miscibility is achieved [6]. In order to improve reservoir recovery, the impact of carbon dioxide gas flooding on recovery has become a hot research topic [7].

At present, research on carbon dioxide flooding for enhanced oil recovery has yielded some results. Varfolomeev et al. studied the oil field production method of advanced water injection and direct injection. Taking the Weibei Oilfield as the research object, they carried out indoor experiments on ultra-low permeability reservoir cores and studied water flooding and carbon dioxide based on nuclear magnetic resonance data. The microscopic oil displacement mechanism of water flooding, conversion from water flooding to gas injection, etc., is concluded. The water flooding oil displacement efficiency in the Weibei ultra-low permeability reservoir is the lowest, only 36%, and the carbon dioxide oil flooding efficiency reaches 55%. The oil displacement efficiency of water flooding to gas flooding is the highest, reaching 60%, so the oil displacement efficiency of water flooding to carbon dioxide injection is the best [8]. Pal et al. studied the effect of carbon dioxide flooding, analyzed the displacement characteristics of carbon dioxide injection in tight oil reservoirs from a micro-scale, and concluded that carbon dioxide flooding effectively activates the crude oil stored in tight pores, and carbon dioxide breaks through quickly under a pressure of 10 MPa. The crude oil in the small pores did not move. Under the pressure of 24 MPa, the breakthrough of carbon dioxide gradually slowed down, the oil saturation decreased linearly after displacement, the oil in the pores was activated, and the recovery rate was high [9]. Ansari et al. studied the changes in the physical properties of crude oil and rocks through the effects of gas injection and expansion of crude oil and formation water dissolution of gas on the characteristics of the reservoir rocks. They concluded that after the injection of carbon dioxide, the viscosity and density of the reservoir crude oil gradually decreased. The volume of crude oil expanded to 45%, and the permeability of oil and gas was 6.5% higher than that of oil and water. Heavy components such as C16-C35 in crude oil gradually increased, and the asphaltene content reached 86%. After carbon dioxide was injected into the reservoir, it gradually dissolved in the formation water so that under the action of weakly acidic formation water, the permeability and porosity of the reservoir gradually increased, and the seepage capacity continued to become stronger [10]. Novak et al. studied the impact of carbon dioxide flooding on the recovery of fault block oil reservoirs. By developing a three-dimensional geological model of fault block oil reservoirs, they simulated the geomorphology of the oil reservoir and used phase analysis software to construct a fault block reservoir geomorphology. Based on the physical property model of the block oil reservoir and conducted carbon dioxide oil displacement experiments, it was concluded that the recovery effect at a well spacing of 250 m is relatively good. When the seepage pressure exceeds 30 MPa, the oil displacement efficiency is high, and the produced gas-oil ratio is the highest [11]. Yan et al. studied the impact of carbon dioxide flooding on the production of the ultra-low permeability Changqing Oilfield. Due to the low production efficiency of early water flooding, the development production was declining year by year. Through carbon dioxide flooding, the daily liquid production volume and daily oil production of the oil wells were increased. The amount has increased significantly, and the water content is gradually decreasing; compared with the water flooding injection pressure, the carbon dioxide injection pressure has not increased significantly and does not change with the injection amount, indicating that the reservoir has good carbon dioxide injection and good air-absorbing capabilities [12].

Judging from the recovery degree, the recovery degree of the homogeneous section is high, reaching 59.53%, but it is necessary to carry out tertiary oil recovery because of the thick reservoir and large remaining oil reserves in the homogeneous section [13].

After carbon dioxide displacement measures are implemented in reservoirs, there are four mechanisms for the change of rock wettability, namely, adsorption and flocculation of asphaltene, ion bridging, repulsion and attraction of net charges, and the influence of formation water.

The exploration of enhanced oil recovery technology by injecting carbon dioxide into a clastic reservoir in the Tarim Oilfield began in 2018. In 2021, in combination with the needs of carbon source conditions, miscible conditions, and the goal of "double carbon," the Tarim Oilfield selected the No.2 well area of the Lunnan Oilfield to carry out pilot tests of carbon dioxide flooding and storage. This practice has proven that carbon dioxide flooding technology can prolong the life of an oil field for more than 10 years, and the cooperative development of oil displacement, extraction, and carbon storage has special advantages. Well No.2 in the Lunnan Oilfield is a realistic potential area for CCUS-EOR development, which has the basis for integrated design of geological engineering.

The Lunnan Oilfield in the Tarim Basin is rich in oil and gas resources and is a tight oil reservoir. Conventional water flooding is difficult to develop, and the recovery rate can be effectively improved by injecting carbon dioxide after water flooding. This paper takes the Lunnan Oilfield in the Tarim Basin as the research object and carries out gas injection expansion, thin tube, long core displacement, oil and gas phase permeability, and solubility laboratory experiments. By injecting carbon dioxide into the formation, the impact of the injection amount of carbon dioxide on the extraction capacity of crude oil, the high-pressure physical property parameters of crude oil, and the phase characteristics of formation fluids were studied. The maximum solubility capacity of carbon dioxide in formation water under different formation temperatures and pressures was analyzed, which provides theoretical support for carbon dioxide flooding to improve oil recovery.

2. Research Methods

2.1. Geological Characteristics

The Tarim Basin is divided into eight first-order structural units, namely, the Kuqa Depression, Tabei Uplift, Northern Depression, Central Uplift, Southwest Depression, Tangguzibasi Depression, Tarnum Uplift, and Southeast Depression from north to south. The structural position of the study area belongs to the Akkule Uplift in the middle part of the Tabei Uplift, also known as the Lunnan Ancient Uplift and the Lunnan Low Uplift. It is bordered by the Luntai Fault in the north, adjacent to the Mangar Depression and the Shuntuoguole Uplift in the south, and the Caohu Depression and the Halahatang Depression in the east and west, respectively. The Lunnan Ancient Uplift covers an area of 4420 km^2 and consists of seven secondary structural units, namely, the northern slope zone, the Lunnan fault barrier zone, the central slope zone, the Santamu fault barrier zone, the southern slope zone, the western slope zone, and the eastern slope zone. Lunnan buried hill was formed by long-term evolution under the control of unified structural conditions of the Tabei Uplift and mainly experienced Gary.

There are four evolutionary stages: the formation period of the Dongbi Uplift, the formation period of the Hercynian anticline, the Indosinian-Yanshan fault activity period, and the Himalayan structure finalization period.

The surface of the Lunnan Oilfield is flat, with an average altitude of about 930 m. Except for the tamarisk and Achnatherum vegetation in a local area, no other plants have been developed [14].

The Lunnan Oilfield belongs to the Lunnan Low Bulge Lunnan Fault Zone tectonics of the Tarim Basin Tabei Uplift. It is an almost east-west trending long-axis anticline, which appears as an irregular skirt extending into the central depression, forming a set of fan delta-braided river delta-lacustrine facies sediments [15]. Well grain size analysis by borehole coring indicates that the lithology of the Lunnan Oil formation is predominantly a medium sandstone composed of quartz, feldspar, lithic debris, and miscellaneous matrix. The rock type is mainly feldspathic lithic sandstone, and the interstitial materials are mainly Kaolinite and mud. The content of potassium feldspar in the reservoir that easily reacts with carbon dioxide is between 9% and 25%. The reservoir sandstone has low compositional maturity and structural maturity [16].

Research has shown that the sand layer group studied in this article belongs to the subfacies of discernible delta plain, with the development of braided distributary channels and channel sand bar sedimentary microfacies. Sandstone is currently in the early stage of diagenesis B to the early stage of the late stage of diagenesis A, with the late stage of diagenesis A being the main stage. Residual intergranular pores and dissolution pores are the main spaces for oil and gas accumulation, with strong intra-layer and planar heterogeneity and weak interlayer heterogeneity. It is a typical medium porosity and medium permeability reservoir. The reservoir evaluation results indicate that the main reservoir types are Class II (good) reservoirs with medium to fine throats, followed by Class I (good) reservoirs with large to coarse throats and large to medium to fine throats, and Class III (medium) reservoirs with small to medium throats.

Injecting CO_2 into the formation to form weak acids can improve the permeability of the reservoir by interacting with rocks such as calcite. In sandstone reservoirs, CO_2 reacts to form precipitates such as kaolinite and clay minerals, which can also block pore throats and cause damage to the reservoir. When the temperature is high, the viscosity of crude oil will decrease, and the solubility of CO_2 in crude oil will also decrease, making it less prone to phase mixing. When the temperature is lower, the higher the viscosity of crude oil, the greater the seepage resistance, and the more severe the fingering phenomenon during the displacement process. The solubility of CO_2 will increase with the increase of reservoir pressure, and the lower the interfacial tension between oil and gas, the easier it is for mixing to occur. The oil displacement efficiency will also increase with the enhancement of CO_2 extraction capacity for light hydrocarbons.

The crude oil Lunnan Oilfield has good properties with low viscosity, low freezing point, low-medium sulfur content, high wax content, and medium colloid asphaltene; the methane content in natural gas is low, with a maximum of 88% and generally 60~84%; the salinity of formation water is 1.9×10^5 mg/L, the chloride ion content is 1.1×10^5 mg/L, and the formation water type is $CaCl_2$ type. Table 1 shows the fluid properties of the Lunnan Oilfield reservoir [16].

Table 1. Reservoir fluid properties of the Lunnan Oilfield.

Crude Oil							Natural Gas		Formation Water	
Ground Density (g/cm^3)	Initial Boiling Point (°C)	Viscosity 50 °C(mPa.s)	Wax Content (%)	Sulfur Content (%)	Freezing Point (°C)	Colloidal Asphal-tene (%)	Proportion (g/cm^3)	Methane Content (%)	Total Min-eralization (10^5 mg/L)	Chloride Ion Content (10^5 mg/L)
0.8632	79.77	13.41	7.0	0.53	−14.1	13.69	0.6919	78.23	1.9	1.1

The experimental cores in this paper were selected from the JIV1 sandstone reservoir core in the central depression of the Lunnan Oilfield in the Tarim Basin, and the depths of the cores ranged from 4554 m to 4583 m (See Table 2).

Table 2. Core parameter table of different injection pressure displacement experiments.

Core Number	Length (cm)	Diameter (cm)	Porosity (%)
1	5.06	2.48	19.38
2	5.73	2.51	14.51
3	5.05	2.52	16.65
4	4.83	2.47	17.80
5	5.29	2.53	15.60
6	7.08	2.51	16.52
7	7.25	2.49	17.23

2.2. Experimental Methods

The experiment adopts the national standard "Oil and Gas Reservoir Fluid Physical Property Analysis Method" [17]; the experimental instrument adopts the oil and gas reservoir fluid analysis instrument, the maximum pressure can reach 150 MPa, and the maximum temperature is 200 °C (See Figure 1).

Figure 1. Oil and gas reservoir fluid analysis instrument.

Experiment procedure:

(1) In the experiment, the temperature was set to 128 °C, the pressure was set to 45.4 MPa, pure carbon dioxide was used as the injection gas, and on-site formation water was used as the water sample. By transferring an appropriate amount of mixed oil samples into a high-temperature and high-pressure sampler and adding excess carbon dioxide, the temperature is kept constant at the formation temperature, the pressure is kept at the bubble point pressure, and the oil is stabilized after sufficient stirring [18]. The excess carbon dioxide from the upper part of the sampler is discharged under constant pressure. The fluid in the sampler is the formation of a crude oil sample, which is used to carry out experiments.

(2) During the experiment, the pressure and temperature data in the reaction kettle were continuously collected and recorded through a data collector. At the same time, the flow rate of carbon dioxide gas and the time of chemical reaction were recorded. Based on the data collected from the experiment, physical parameters such as density and viscosity of carbon dioxide gas are calculated.

(3) After extracting and drying the core, measure the gas permeability of the core, sort them in order according to the permeability, connect the core model, and measure the porosity of the saturated formation water in the core model. Oil is injected into the water-saturated core to drive water with oil until there is no water flow at the outlet of the core, and the irreducible water saturation of the core model is calculated.

(4) Connect the cylinder to the container to ensure that the gas enters the container smoothly. Set a pressure sensor and a temperature sensor on the cylinder, connect it to the back pressure valve at the outlet end of the core, and add a predetermined pressure; adjust a certain displacement pressure, and carbon dioxide gas is injected into the core to conduct carbon dioxide gas flooding tight oil experiments until no more crude oil is produced at the outlet end, thereby measuring the cumulative volume of displaced oil and gas and the cumulative volume of injected gas.

(5) Pump the formation oil into the thin tube core until no water comes out from the outlet end, and calculate the irreducible water saturation and original oil saturation in the thin tube model; maintain the back pressure during the experiment, determine

the displacement pressure, conduct the displacement experiment under a certain displacement pressure, and record the pump volume and oil production parameters.

(6) By changing the displacement pressure and repeating the experiment, the gas drive recovery rate under different displacement pressures is measured. The minimum pressure corresponding to the gas drive recovery rate of 90–95% is recorded as the minimum miscible pressure [19].

(7) Place the core sample in the permeability measuring device to ensure that the sample can seep smoothly. A pressure sensor and a temperature sensor are provided on the permeability measurement device to monitor pressure and temperature changes during the seepage process.

(8) In the experiment, the permeability was set to 0.1 mD~1000 mD, the porosity was 5~30%, and the pressure gradient was set to 0.1 MPa/m~10 MPa/m. Oil and gas were injected from the oil and gas source into the core sample, and the pressure sensors and temperature sensors monitor the pressure and temperature of oil and gas, and the flow meter monitors the seepage rate of oil and gas. At the same time, data such as the permeability, pressure, and temperature of oil and gas in core samples are continuously collected, and the injection time and amount of oil and gas are recorded through a data collector.

(9) Put the prepared solution into a constant temperature bath, heat it to the set temperature, and stir the solution with a magnetic stirrer to ensure uniformity of the solution; during the dissolution process, monitor the solution in real-time with a pH meter and conductivity meter and monitor the concentration changes of dissolved substances in the solution through spectrophotometer and other instruments, and continuously collect and record the concentration, pH value, conductivity, dissolution time and amount of dissolved substances in the solution (See Figure 2).

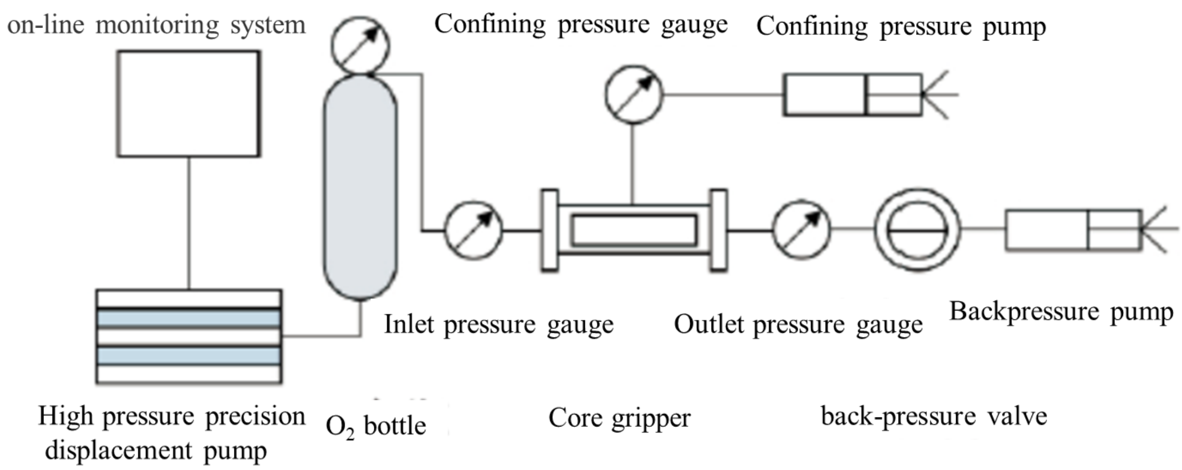

Figure 2. Flow chart of saturated crude oil core displacement experiment.

3. Results

3.1. High-Temperature and High-Pressure Physical Properties of Carbon Dioxide

By recording the physical property changes of carbon dioxide under different temperatures and pressures, the high-temperature and high-pressure physical properties of carbon dioxide under reservoir conditions are determined. Table 3 shows the crude oil sampling results of the Lunnan oil group. It can be seen from Table 3 that under oil group conditions, the density of carbon dioxide is 0.74 g/cm^3, which is basically close to the density of crude oil, but its viscosity is 0.0681 mPa·s, which improves the mobility ratio of crude oil and has good adaptability to carbon dioxide flooding [20]. Through a chromatographic analysis of the oil and gas sample composition and well flow composition, the well flow composition of the formation fluid and the single-degassing experimental data were obtained (Table 4).

Table 3. Lunnan oil group crude oil sampling results.

Gas/Oil Ratio (m^3/m^3)	Coefficient of Expansion	Volume Coefficient	Bubble Point Pressure (MPa)	Crude Oil Density (g/cm^3)	Crude Oil Viscosity under Formation Pressure (mPa·s)
42.52	1	1.14	12.06	0.79	3.6

Table 4. Formation fluid well flow components composition.

Component Name	Well Flow Molar Composition (%)	Component Name	Well Flow Molar Composition (%)
N_2	1.15	nC_4	1.73
carbon dioxide	0.88	iC_5	1.34
C_1	29.89	nC_5	1.36
C_2	2.15	C_6	4.40
C_3	1.33	C_{7+}	55.11
iC_4	0.64	C_{7+} molecular weight	362.20

3.2. Gas Injection Expansion Characteristics

By transferring the prepared formation fluid sample into the PVT instrument, after the formation temperature stabilizes for 2 h, add an appropriate amount of pressurized formation crude oil sample and stir it thoroughly for 2 h to make the sample into a homogeneous single-phase state. Then, slowly reduce the pressure, measure its bubble point, and perform a single removal test to test the amount of dissolved gas in crude oil and the density and viscosity of the fluid [21]. After the test is completed, continue to inject carbon dioxide into the oil sample according to the above experimental method, increase stirring to make the sample into a homogeneous single-phase state, then reduce the pressure to measure its new bubble point and conduct a single removal test. Through multiple consecutive additions of injected gas, the gas injection expansion results of the Lunnan Oilfield formation were obtained (See Table 5).

Table 5. Gas injection expansion results of formations in the Lunnan Oilfield.

Injected Gas Mole Fraction (Decimal)	Gas/Oil Ratio (m^3/m^3)	Coefficient of Expansion	Volume Coefficient	Saturation Pressure (MPa)	Surface Degassed Crude Oil Density (g/cm^3)	Viscosity under Formation Pressure (mPa·s)
0	42.52	1	1.14	12.06	0.79	3.62
0.39	126.63	1.1	1.34	19.72	0.81	1.98
0.56	206.56	1.2	1.52	25.50	0.82	1.48
0.67	316.56	1.3	1.76	30.65	0.82	1.27
0.82	594.68	1.4	2.37	39.68	0.82	1.05

As the amount of injected carbon dioxide increases, the saturation pressure of crude oil increases from 12.06 MPa to 39.68 MPa, and the gas-oil ratio increases from 42.52 m^3/m^3 to 594.68 m^3/m^3, indicating that the sample has a strong impact on carbon dioxide. The dissolving ability of crude oil is strong. As the pressure increases, carbon dioxide will quickly dissolve into crude oil, and its gas-oil ratio, expansion coefficient, and saturation pressure will gradually increase. Due to the dissolved carbon dioxide in crude oil and the extraction of crude oil by carbon dioxide, the viscosity gradually decreased from 3.62 mPa·s to 1.05 mPa·s, and the expansion coefficient increased from 1 to 1.4. Therefore, after carbon dioxide is injected into the oil reservoir, it achieves good expansion and viscosity reduction effects.

3.3. Minimum Miscibility Pressure

This article uses configured formation fluid samples to test the minimum miscible pressure of carbon dioxide and formation crude oil to determine whether the reservoir has achieved miscible carbon dioxide flooding. The degree of recovery is achieved by injecting gas under different experimental pressures [22]. Figure 3 shows the degree of CO_2 flooding recovery under different pressures. As the displacement pressure continues to decrease, the degree of carbon dioxide displacement decreases slowly at first and then decreases rapidly. When the displacement pressure exceeds 27.5 MPa, the degree of carbon dioxide displacement exceeds 90%. Therefore, the minimum miscible pressure for carbon dioxide injection is 27.35 MPa. However, the current formation pressure is 49.88 MPa, which can achieve the miscibility of carbon dioxide and the formation of crude oil.

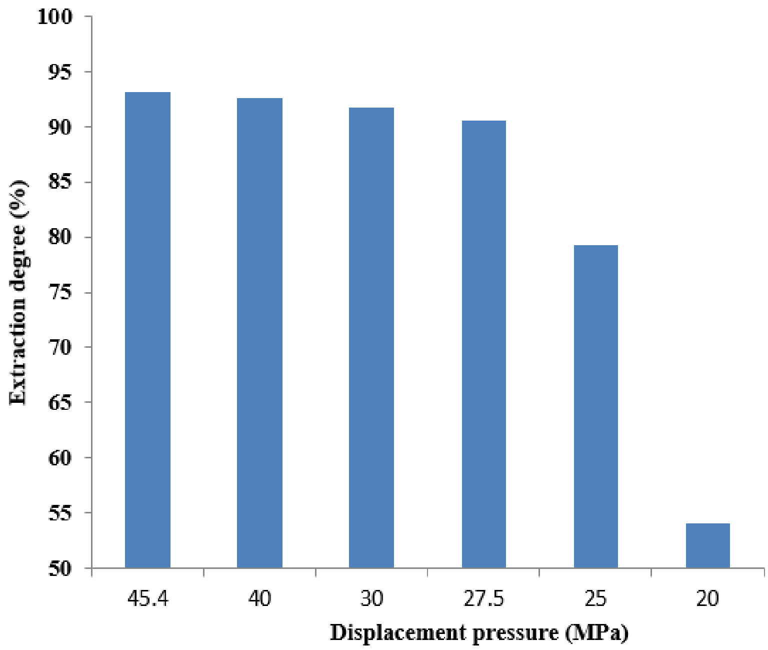

Figure 3. Carbon dioxide injection and recovery degree under different pressures.

3.4. Long Core Displacement Characteristics

In this paper, core samples with a length of 6 cm were spliced to prepare cores of the required length and filter paper was placed between two adjacent cores to effectively reduce the end effect [23]. In order to characterize the physical properties and water content of the Lunnan oil reservoir, a long core displacement experiment was conducted by testing the porosity and permeability data of the core. The displacement experiments of continuous gas flooding after water flooding, water and gas alternation, periodic gas injection, and carbon dioxide + hydrocarbon gas slug were completed. The core length of the Lunnan Oil Formation water flooding followed by different displacement methods of carbon dioxide injection is 100 cm, the diameter is 3.8 cm, the permeability is 45 mD, and the porosity is 17%. Taken from wild outcrops, they are prepared by bonding, pressing, and wire cutting. Figure 4 shows the long core displacement experimental core of carbon dioxide injected after water flooding in the Lunnan Oil Formation.

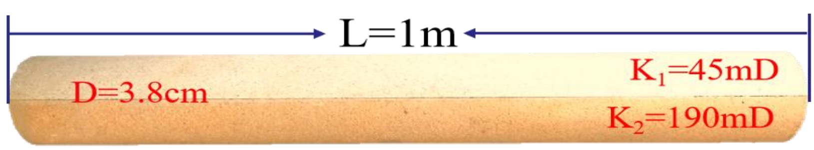

Figure 4. Carbon dioxide injection long core displacement experimental core after water flooding in the Lunnan Oil Formation.

The long core displacement experimental results were obtained through continuous carbon dioxide gas injection (See Figure 5). After water flooding in the Lunnan oil formation, as the injection rate of carbon dioxide pore volume increases, the displacement efficiency increases first rapidly and then slowly, with a turning point of 0.8 HCPV. The gas-oil ratio increased slowly at first and then rapidly, with the turning point being 0.6 HCPV.

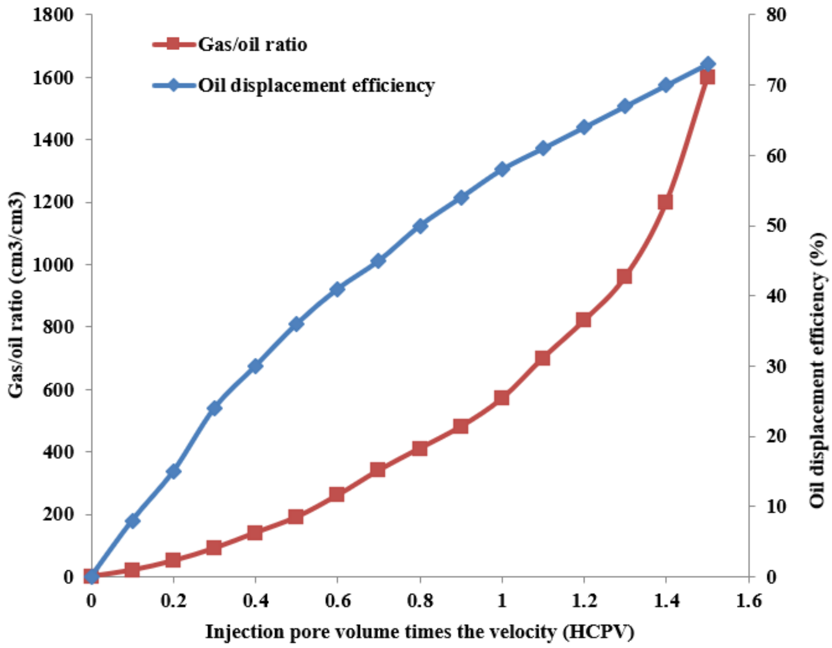

Figure 5. Experimental results of continuous carbon dioxide gas flooding after water flooding in the Lunnan Oil Formation.

A new and accurate calculation method has been proposed to predict the vapor-liquid equilibrium of CO_2 binary mixtures, which is not entirely dependent on experimental data [24]. Carbon capture and storage (CCS) has become a promising way to solve this challenge. It is estimated that in heavy industry, CCS can reduce emissions by 25–67% [25]. The saltwater layer has a CO_2 injection well and 200 GRs, which have different uncertain petrophysical characteristics. UML framework can be used to select RGRs and capture the whole uncertain domain. The calculation cost related to scheme testing, decision-making, and development planning of CO_2 storage sites under geological uncertainty is significantly reduced [26]. The carbon dioxide flooding in this paper can also achieve the purpose of carbon sequestration.

3.5. Oil and Gas Phase Permeability Characteristics

Based on the expansion experiment, thin tube experiment, and long core displacement experiment, the phase permeability characteristics of carbon dioxide injection gas flooding in the reservoir were obtained. Table 6 shows the characteristics of the reservoir fluid components. During the carbon dioxide flooding process, miscibility, mass transfer, extraction, expansion, and other functions greatly increase the fluidity of crude oil. The water flooding efficiency of the Lunnan oil formation is close to the limit. After conversion to carbon dioxide flooding development, on the one hand, the co-permeability interval is increased, and the fluidity of crude oil is increased; on the other hand, the residual oil saturation and irreducible water saturation are further reduced, releasing the movable space for oil, gas, and water, and the residual oil saturation is reduced from 30% to 12%.

Table 6. Reservoir fluid component characteristics.

Components Name	Molecular Weight (g/mol)	Equation Coefficient	Equation Coefficient	Critical Temperature (K)	Critical Pressure (b)	Critical Volume	Critical Z Factor	Volume Offset Coefficient	Eccentric Factor
N_2	28.01	0.45	0.078	126.20	33.50	90.00	0.29	−0.13	0.04
CO_2	44.01	0.45	0.078	320.08	102.96	94.00	0.36	0	0.34
C_1	16.04	0.45	0.078	277.00	212.70	98.00	0.91	−0.022	0.0055
C_2~C_5	53.34	0.45	0.078	397.86	39.43	237.45	0.28	−0.065	0.18
C_6~C_{10}	110.76	0.45	0.078	578.48	35.15	447.39	0.33	0.0	0.32
C_{11+}	180.03	0.45	0.078	666.99	23.52	728.18	0.31	0.0001	0.58
C_{17+}	365.77	0.45	0.078	859.91	12.43	1458.12	0.25	0.0002	1.09

Completely miscible CO_2 displacement can well displace various components of crude oil, including heavy components, and the difference of oil sample family components in different displacement stages is very small, and the miscible effect is excellent. After CO_2 flooding with large injection, the heavy components in the ultra-low permeability tight reservoir are well recovered, and the final recovery degree of heavy components is similar to that in the medium and low permeability reservoir, which shows that CO_2 flooding with large injection is a practical and effective displacement scheme to improve the recovery degree of ultra-low permeability tight reservoir. This makes CO_2 flooding very suitable for oil displacement and exploitation in the Lunnan Oilfield.

3.6. Water Solubility Characteristics

By obtaining aqueous solutions containing supersaturated carbon dioxide under different pressures and carrying out a single degassing experiment on saturated carbon dioxide water samples after the pressure stabilizes, the ability of water samples to dissolve carbon dioxide under different pressure conditions is measured. Figure 6 shows the variation pattern of sample solubility with pressure. The solubility of carbon dioxide in water increases with the increase of pressure, basically showing a linear relationship. Under the current formation pressure conditions, the solubility of carbon dioxide in formation water is 24 m^3/m^3.

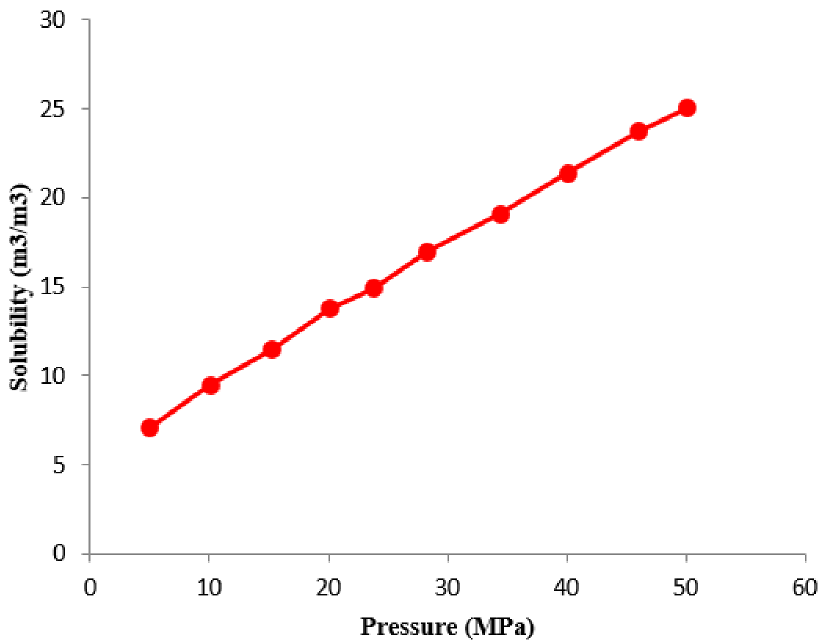

Figure 6. Solubility changes with pressure.

After carbon dioxide displacement, the wettability of reservoir rocks turns to be lipophilic. Most of the actual reservoirs are strongly hydrophilic, but after carbon dioxide displacement, the reservoirs can become weakly hydrophilic. After the injection of dissolved CO_2, the reservoir pressure and the reservoir pressure impact range continuously increase. After the injection is stopped, the reservoir pressure quickly recovers to its original value, ensuring the feasibility and safety of dissolved CO_2 storage. The pH value is mainly affected by pressure, water–rock reactions, and diffusion. Injecting dissolved CO_2 can preserve the reservoir for a long time, ensuring safety. Illite minerals undergo dissolution, while kaolinite minerals undergo precipitation. The total dissolution of minerals in the reservoir near the injection well is greater than the total precipitation, which increases the porosity of the reservoir. In the later stage of injection, the porosity of various positions in the reservoir no longer changes. The increase in reservoir porosity increases the permeability of the reservoir, alleviates the increase in reservoir pressure, and ensures the feasibility and safety of dissolved CO_2 storage.

4. Discussion

The heterogeneity of continental reservoirs in China is strong, and the fractures in low permeability reservoirs are developed. At the same time, the types of reservoirs in China are complex, and they are difficult to develop. The research of CO_2 oil recovery technology in China started late, and it was not until the end of the 1950s that China began to study the topic of CO_2 flooding. Then, in 1963, China first conducted research on enhancing oil recovery by CO_2 flooding in the Daqing Oilfield and then conducted the pilot tests of CO_2 injection in 1966 and 1969, respectively. In 1980, the pilot test of CO_2 miscible flooding was carried out in the Shaxia Reservoir of Pucheng Oilfield, and the purpose of dewatering flooding was achieved. CO_2 flooding is developing rapidly. In 2014, CO_2 flooding was carried out in the Jingbian Oilfield, a typical low-permeability reservoir. The final results show that CO_2 water-gas alternation can make the oil displacement efficiency reach 77.3%, and a stable production increase can be achieved by using CO_2 flooding technology.

In this paper, the study of CO_2 flooding, the determination of minimum miscible pressure in the Lunnan sandstone reservoir in the Tarim Basin, the study of reservoir fluid phase state after CO_2 injection, and the feasibility of CO_2-EOR technology is possible because injected carbon dioxide can reduce the viscosity of crude oil, increase the fluidity of crude oil, reduce the interfacial tension between oil and water, and expand the volume of crude oil, thus improving the oil recovery. The conclusion of this experiment is that with the increase in pressure, the injection capacity of CO_2 increases. The injection capacity of CO_2 is much greater than that of water injection. Compared with water injection, pure CO_2 flooding can improve oil recovery.

5. Conclusions

Injecting carbon dioxide under current formation pressure conditions, the impact of different amounts of carbon dioxide injection on crude oil extraction capacity, high-pressure physical properties of crude oil, and formation fluid phase characteristics varies. The following conclusions are ultimately drawn:

(1) The crude oil from the Lunnan Oilfield has low viscosity, low solidification point, low medium sulfur content, high wax content, and medium colloidal asphaltene. The carbon dioxide density measured under oil group conditions is 0.74 g/cm^3, which is similar to the density of crude oil. But its viscosity is 0.0681 mPa·s, which has good applicability for carbon dioxide flooding.

(2) As the amount of carbon dioxide injected increases, the saturation pressure of crude oil increases from 12.06 MPa to 39.68 MPa. The gas–oil ratio has increased from 42.52 m^3/m^3 to 594.68 m^3/m^3. The gas–oil ratio, expansion coefficient, and saturation pressure gradually increase. As the displacement pressure continues to decrease, the carbon dioxide displacement efficiency begins to slowly decrease and then rapidly decline. As the injection rate of carbon dioxide pore volume increases, the growth rate first increases and then slows down, reaching a turning point at 0.8 HCPV., The oil–gas ratio also exhibits a turning point occurring at 0.6 HCPV. The solubility of

carbon dioxide in the formation of water is determined to be 24 m^3/m^3. Beneficial for subsequent oil recovery and carbon storage.

Author Contributions: Conceptualization, Z.W.; Methodology, Q.F., Y.T., D.Z. and L.L.; Software, Z.W., Q.F. and Y.T.; Validation, Z.W., Y.T., D.Z. and L.L.; Formal analysis, Z.W., Q.F. and Y.T.; Investigation, Z.W., Y.T. and D.Z.; Resources, Z.W., Q.F. and D.Z.; Data curation, Z.W., Q.F. and L.L.; Writing – original draft, Z.W., Q.F., Y.T., D.Z. and L.L.; Writing – review & editing, Z.W., Q.F., Y.T., D.Z. and L.L.; Project administration, Q.F. All authors have read and agreed to the published version of the manuscript.

Funding: This work was supported by Major Science and Technology Project of CNPC (Grant No. ZD2019-183-007).

Data Availability Statement: The figures and tables used to support the findings of this study are included in the article.

Acknowledgments: The authors would like to show sincere thanks to those techniques who have contributed to this research.

Conflicts of Interest: Author Zangyuan Wu, Yongliang Tang and Daiyu Zhou were employed by the company PetroChina Tarim Oilfield Company. The remaining authors declare that the research was conducted in the absence of any commercial or financial relationships that could be construed as a potential conflict of interest. The authors declare that they have no known competing financial interests or personal relationships that could have appeared to influence the work reported in this paper. Author Zangyuan Wu, Yongliang Tang and Daiyu Zhou are employee of CNPC, who provided funding and teachnical support for the work. The funder had no role in the design of the study; in the collection, analysis, or interpretation of data, in the writing of the manuscript, or in the decision to publish the results.

References

1. Al-Obaidi, D.A.; Al-Mudhafar, W.J.; Al-Jawad, M.S. Experimental evaluation of Carbon Dioxide-Assisted Gravity Drainage process (CO_2-AGD) to improve oil recovery in reservoirs with strong water drive. *Fuel* **2022**, *324*, 124409. [CrossRef]
2. Guerra, A.; McElligott, A.; Du, C.Y.; Marić, M.; Rey, A.D.; Servio, P. Dynamic viscosity of methane and carbon dioxide hydrate systems from pure water at high-pressure driving forces. *Chem. Eng. Sci.* **2022**, *252*, 117282. [CrossRef]
3. Liu, M.; Yang, X.; Wen, J.; Wang, H.; Feng, Y.; Lu, J.; Wang, J. Drivers of China's carbon dioxide emissions: Based on the combination model of structural decomposition analysis and input-output subsystem method. *Environ. Impact Assess. Rev.* **2023**, *100*, 107043. [CrossRef]
4. Kalam, S.; Olayiwola, T.; Al-Rubaii, M.M.; Amaechi, B.I.; Jamal, M.S.; Awotunde, A.A. Carbon dioxide sequestration in underground formations: Review of experimental, modeling, and field studies. *J. Pet. Explor. Prod.* **2021**, *11*, 303–325. [CrossRef]
5. Lv, Z.; Qiao, K.; Chu, F.; Yang, L.; Du, X. Experimental study of divalent metal ion effects on ammonia escape and carbon dioxide desorption in regeneration process of ammonia decarbonization. *Chem. Eng. J.* **2022**, *435*, 134841. [CrossRef]
6. Sun, X.; Cai, J.; Li, X.; Zheng, W.; Wang, T.; Zhang, Y. Experimental investigation of a novel method for heavy oil recovery using supercritical multithermal fluid flooding. *Appl. Therm. Eng.* **2021**, *185*, 116330. [CrossRef]
7. Chuah, L.F.; Bokhari, A.; Asif, S.; Klemeš, J.J.; Dailin, D.J.; El Enshasy, H.; Yusof, A.H.M. A review of performance and emission characteristic of engine diesel fuelled by biodiesel. *Chem. Eng. Trans.* **2022**, *94*, 1099–1104.
8. Varfolomeev, M.A.; Yuan, C.; Bolotov, A.V.; Minkhanov, I.F.; Mehrabi-Kalajahi, S.; Saifullin, E.R.; Shaihutdinov, D.K. Effect of copper stearate as catalysts on the performance of in-situ combustion process for heavy oil recovery and upgrading. *J. Pet. Sci. Eng.* **2021**, *207*, 109125. [CrossRef]
9. Pal, N.; Zhang, X.; Ali, M.; Mandal, A.; Hoteit, H. Carbon dioxide thickening: A review of technological aspects, advances and challenges for oilfield application. *Fuel* **2022**, *315*, 122947. [CrossRef]
10. Ansari, K.B.; Gaikar, V.G.; Trinh, Q.T.; Khan, M.S.; Banerjee, A.; Kanchan, D.R.; Danish, M. Carbon dioxide capture over amine functionalized styrene divinylbenzene copolymer: An experimental batch and continuous studies. *J. Environ. Chem. Eng.* **2022**, *10*, 106910. [CrossRef]
11. Novak Mavar, K.; Gaurina-Međimurec, N.; Hrnčević, L. Significance of enhanced oil recovery in carbon dioxide emission reduction. *Sustainability* **2021**, *13*, 1800. [CrossRef]
12. Yan, H.; Zhang, J.; Li, B.; Zhu, C. Crack propagation patterns and factors controlling complex crack network formation in coal bodies during tri-axial supercritical carbon dioxide fracturing. *Fuel* **2021**, *286*, 119381. [CrossRef]
13. Zhou, M.; Feng, J.; Jiang, T.; Liu, J. Preliminary study on tertiary oil recovery of high temperature and high salinity reservoirs in Tarim Oilfield. *Xinjiang Pet. Geol.* **2010**, *2*, 59–62.

14. Wen, B.; Shi, Z.; Jessen, K.; Hesse, M.A.; Tsotsis, T.T. Convective carbon dioxide dissolution in a closed porous medium at high-pressure real-gas conditions. *Adv. Water Resour.* **2021**, *154*, 103950. [CrossRef]
15. Bagheri, H.; Hashemipour, H.; Rahimpour, E.; Rahimpour, M.R. Particle size design of acetaminophen using supercritical carbon dioxide to improve drug delivery: Experimental and modeling. *J. Environ. Chem. Eng.* **2021**, *9*, 106384. [CrossRef]
16. Wang, Y.; Dong, Y.; Zhang, L.; Chu, G.; Zou, H.; Sun, B.; Zeng, X. Carbon dioxide capture by non-aqueous blend in rotating packed bed reactor: Absorption and desorption investigation. *Sep. Purif. Technol.* **2021**, *269*, 118714. [CrossRef]
17. Ringrose, P.S.; Furre, A.K.; Gilfillan, S.M.; Krevor, S.; Landrø, M.; Leslie, R.; Zahid, A. Storage of carbon dioxide in saline aquifers: Physicochemical processes, key constraints, and scale-up potential. *Annu. Rev. Chem. Biomol. Eng.* **2021**, *12*, 471–494. [CrossRef]
18. Yang, L.; Wang, Y.; Lian, Y.; Dong, X.; Liu, J.; Liu, Y.; Wu, Z. Rational planning strategies of urban structure, metro, and car use for reducing transport carbon dioxide emissions in developing cities. *Environ. Dev. Sustain.* **2023**, *25*, 6987–7010. [CrossRef]
19. Mao, F.; Li, Z.; Zhang, K. A comparison of carbon dioxide emissions between battery electric buses and conventional diesel buses. *Sustainability* **2021**, *13*, 5170. [CrossRef]
20. Vaz, S., Jr.; de Souza, A.P.R.; Baeta, B.E.L. Technologies for carbon dioxide capture: A review applied to energy sectors. *Clean. Eng. Technol.* **2022**, *8*, 100456. [CrossRef]
21. Lyu, Q.; Tan, J.; Li, L.; Ju, Y.; Busch, A.; Wood, D.A.; Hu, R. The role of supercritical carbon dioxide for recovery of shale gas and sequestration in gas shale reservoirs. *Energy Environ. Sci.* **2021**, *14*, 4203–4227. [CrossRef]
22. Jia, W.; Jia, X.; Wu, L.; Guo, Y.; Yang, T.; Wang, E.; Xiao, P. Research on regional differences of the impact of clean energy development on carbon dioxide emission and economic growth. *Humanit. Soc. Sci. Commun.* **2022**, *9*, 25. [CrossRef]
23. Voumik, L.C.; Ridwan, M.; Rahman, M.H.; Raihan, A. An investigation into the primary causes of carbon dioxide releases in Kenya: Does renewable energy matter to reduce carbon emission? *Renew. Energy Focus* **2023**, *47*, 100491. [CrossRef]
24. Motie, M.; Bemani, A.; Soltanmohammadi, R. On The Estimation of Phase Behavior Of CO_2-Based Binary Systems Using ANFIS Optimized By GA Algorithm. In *Fifth CO_2 Geological Storage Workshop*; European Association of Geoscientists & Engineers: Utrecht, The Netherlands, 2018; Volume 2018, pp. 1–5.
25. Mahjour, S.K.; Faroughi, S.A. Risks and uncertainties in carbon capture, transport, and storage projects: A comprehensive review. *Gas Sci. Eng.* **2023**, *119*, 205117. [CrossRef]
26. Mahjour, S.K.; Faroughi, S.A. Selecting representative geological realizations to model subsurface CO_2 storage under uncertainty. *Int. J. Greenh. Gas Control.* **2023**, *127*, 103920. [CrossRef]